

Cation Exchange Strategy for the Encapsulation of a Photoactive CO-Releasing Organometallic Molecule into Anionic Porous Frameworks

Francisco J. Carmona,[†] Sara Rojas,[†] Purificación Sánchez,[†] Hélia Jeremias,[‡] Ana R. Marques,[§] Carlos C. Romão,^{‡,§} Duane Choquesillo-Lazarte,^{||} Jorge A. R. Navarro,[†] Carmen R. Maldonado,^{*,†} and Elisa Barea^{*,†}

[†]Department of Inorganic Chemistry, University of Granada, Av. Fuentenueva S/N, 18071 Granada, Spain

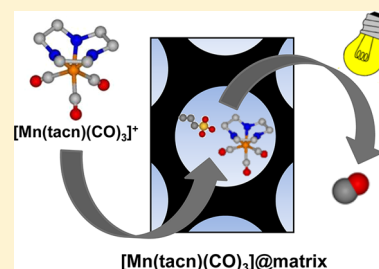
[‡]Instituto de Tecnologia Química e Biológica da Universidade Nova de Lisboa, Av. da República, EAN, 2780-157 Oeiras, Portugal

[§]Alfama Ltd., Instituto de Biologia Experimental e Tecnológica, IBET, Av. da República, EAN, 2780-157 Oeiras, Portugal

^{||}Laboratorio de Estudios Cristalográficos, IACT-CSIC, Av. de las Palmeras, 4, 18100 Armilla, Granada, Spain

Supporting Information

ABSTRACT: The encapsulation of the photoactive, nontoxic, water-soluble, and air-stable cationic CORM $[\text{Mn}(\text{tacn})(\text{CO})_3]\text{Br}$ ($\text{tacn} = 1,4,7\text{-triazacyclononane}$) in different inorganic porous matrixes, namely, the metalorganic framework bio-MOF-1, $(\text{NH}_2(\text{CH}_3)_2)_2[\text{Zn}_8(\text{adeninate})_4(\text{BPDC})_6] \cdot 8\text{DMF} \cdot 11\text{H}_2\text{O}$ ($\text{BPDC} = 4,4'\text{-biphenyldicarboxylate}$), and the functionalized mesoporous silicas MCM-41- SO_3H and SBA-15- SO_3H , is achieved by a cation exchange strategy. The CO release from these loaded materials, under simulated physiological conditions, is triggered by visible light. The results show that the silica matrixes, which are unaltered under physiological conditions, slow the kinetics of CO release, allowing a more controlled CO supply. In contrast, bio-MOF-1 instability leads to the complete leaching of the CORM. Nevertheless, the degradation of the MOF matrix gives rise to an enhanced CO release rate, which is related to the presence of free adenine in the solution.



INTRODUCTION

Carbon monoxide (CO), typically released in car exhaust gases, is known as the silent killer because of its toxicity to humans and animals at medium to high concentrations. Despite its reputation as a toxic gas, CO is produced naturally in animals and acts as an important cell-signaling molecule, playing an essential role in various important physiological as well as pathological cellular processes, showing cell protective, anti-inflammatory, and vasodilatory effects.^{1,2} On the basis of this knowledge, there is a growing interest in the use of CO as a therapeutic agent by enhancement of endogenous CO production or direct delivery of exogenous CO.^{3,4}

In addition to the main role of endogenous CO as a blood vessel dilator, exogenously applied CO has been shown to produce a beneficial health effect in animal models.⁵ However, the practical clinical use of CO gas is currently hampered, since inhaled CO results in its global vascular distribution due to its strong binding to the hemoglobin of red blood cells, 200 times stronger than to O_2 , creating a formidable barrier to tissue penetration. This limitation outlines the requirement of more efficient methods for the therapeutic delivery of CO to the injury in need of treatment.⁶

One of the methods devised for the specific delivery of exogenous CO to targeted locations is the development of CO-releasing molecules (CORMs). CORMs are mainly organometallic compounds, based on transition-metal carbonyls with one or more CO groups as coordinated ligands. Since the pioneering work of Clark⁷ and the subsequent studies of

Motterlini^{8,9} on the biological application of CORM-3, $[\text{Ru}(\text{CO})_3\text{Cl}(\text{glycinate})]$, numerous CORMs have been synthesized using different transition-metal ions (Mn,^{10–13} Mo,⁴ Fe,¹⁴ Ru,¹⁵ Re,¹⁶ etc.). Preclinical studies have demonstrated that CORMs have anti-inflammatory, antiapoptotic, anti-ischemic, anticarcinogenic, pro-angiogenic, antiaggregatory, and cardioprotective properties,^{7,17–20} and they can inhibit cell proliferation and regulate mitochondrial respiration.²¹ In addition, CORMs have been used in organ transplantation, reducing ischemia-reperfusion injury during organ cold storage.²² Another innovative application is related to the use of photoactive CORMs for topical applications in epidermal cancer treatment. Indeed, CORM-2, $[\text{Ru}_2\text{Cl}_4(\text{CO})_6]$, lotions were shown to reduce acute and chronic inflammation and tumor multiplicity in hairless mice with induced photocarcinogenesis.²³

However, CO-releasing molecules need to meet specific requirements to be used as therapeutic agents, such as (i) stability under ambient conditions, (ii) solubility in physiological media, (iii) controlled CO delivery kinetics, (iv) low toxicity of both CORM itself and its degradation products (metal–coligand fragments), and (v) possible trigger CO liberation.^{19,20,24} For all these reasons, sophisticated strategies are under investigation to achieve the administration of a defined amount of CO, at a predetermined location and time,

Received: March 17, 2016

Published: June 11, 2016

using a CORM as the prodrug. In this regard, the development of solid-storage forms of CO in combination with a specific trigger for the gas release is an important research goal. In particular, CO-releasing materials (CORMs) may represent improved CO-delivering devices, as the CO distribution can be controlled over time and location. However, only a few investigations have reported findings based on CO-releasing materials to date. For example, Hubbell et al.²⁵ have developed a new CORMA by using micellar forms of metal carbonyl complexes as delivery systems and inducing the CO release via a cysteine reaction. Other examples comprise the covalent attachment of the photoactivatable CO-releasing molecule $[\text{Mn}(\text{tpm})(\text{CO})_3]\text{PF}_6$ (tpm = tris(pyrazolyl)methane) to the surface of silica dioxide nanoparticles²⁶ or dopable nano-diamonds.²⁷ Moreover, Janiak et al.²⁸ have prepared biocompatible magnetic iron oxide nanoparticles as carriers for a CORM-3 derivative, leading to the controlled delivery of CO by application of an external alternating magnetic field. More recently, a new CO-releasing material has been designed by embedding the photosensitive CORM-1, $[\text{Mn}_2(\text{CO})_{10}]$, into the nanoporous fibrous nonwovens of polylactic acid.²⁹ In addition, inorganic porous materials, such as zeolites, mesoporous silicas, and metal-organic frameworks (MOFs), can be considered as good candidates as CORMAs. In fact, several works have already shown the promising biological applications of these materials on CO gas adsorption, storage, and delivery.³⁰ It should be noted that the high surface area to volume ratio of these porous matrixes, their ordered networks, and their functionalizable pore walls are excellent features for the incorporation of CORMs in their structures and the subsequent controlled delivery of CO.^{31,32} In this context, Dennis et al.³³ have reported the potential use of devices such as soft tissue implants for inhibiting fibrosis on the basis of the adsorption of nongaseous CO in a zeolite. On the other hand, the photoactive manganese carbonyl complex *fac*- $[\text{Mn}(\text{pqa})(\text{CO})_3]\text{Cl}$ (pqa = (2-pyridylmethyl)(2-quinolylmethyl)amine) has been recently incorporated into the mesoporous silica Al-MCM-41.³⁴ To the best of our knowledge, no other examples regarding the use of inorganic porous materials to encapsulate CORMs have been reported to date.

Taking into account all the above information, here we present the encapsulation of the photoactive, nontoxic, water-soluble, and air-stable cationic CORM $[\text{Mn}(\text{tacn})(\text{CO})_3]\text{Br}$ (tacn = 1,4,7-triazacyclononane),³⁵ also known as ALF472, into different inorganic porous matrixes, namely, the metal-organic framework bio-MOF-1, $(\text{NH}_2(\text{CH}_3)_2)_2[\text{Zn}_8(\text{adeninate})_4(\text{BPDC})_6] \cdot 8\text{DMF} \cdot 11\text{H}_2\text{O}$ (BPDC = 4,4'-biphenyldicarboxylate),³⁶ and the functionalized mesoporous silicas MCM-41- SO_3H ³⁷ and SBA-15- SO_3H ³⁸ (Figure 1), by means of a simple ion exchange strategy. We have selected the above porous materials as they are biocompatible and exhibit anionic frameworks with adequate pore size (0.52, 3.91, and 5.83 nm in bio-MOF-1, MCM-41- SO_3H , and SBA-15- SO_3H , respectively)^{36,39} in which the loading and retention of the cationic CORM $[\text{Mn}(\text{tacn})(\text{CO})_3]^+$ (ALF472⁺) can be optimized by a cation exchange strategy in order to study the kinetics of CO release by activation with visible light.

EXPERIMENTAL SECTION

All chemicals were commercially available and were used without further purification.

Synthesis of $(\text{NH}_2(\text{CH}_3)_2)_2[\text{Zn}_8(\text{adeninate})_4(\text{BPDC})_6] \cdot 8\text{DMF} \cdot 11\text{H}_2\text{O}$ (bio-MOF-1). The porous material bio-MOF-1 was

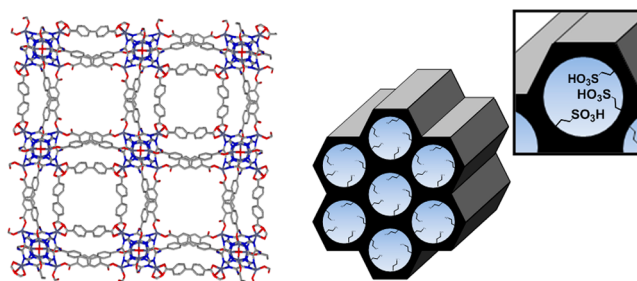


Figure 1. Structures of the selected anionic host matrixes for encapsulation of the cationic $[\text{Mn}(\text{tacn})(\text{CO})_3]^+$ (ALF472) CORM: $(\text{NH}_2(\text{CH}_3)_2)_2[\text{Zn}_8(\text{adeninate})_4(\text{BPDC})_6]$ (bio-MOF-1) (left) and mesoporous silicas SBA-15- SO_3H and MCM-41- SO_3H (right). The inset highlights the alkanesulfonic acid functionalization of the mesoporous silicas.

synthesized as reported.³⁶ In a typical synthesis, a mixture of 16.89 mg (0.125 mmol) of adenine, 60.56 mg (0.25 mmol) of 4,4'-biphenyldicarboxylic acid (H_2BPDC), 82.32 mg (0.375 mmol) of zinc acetate dihydrate, and 42 μL (1 mmol) of nitric acid in DMF (13.5 mL) and deionized water (1 mL), was placed in a 20 mL vial. The vial was capped, and the resulting solution was heated at 130 °C for 24 h. After the reaction time had elapsed, the mixture was centrifuged (4000 rpm/10 min) and washed with DMF (3×10 mL) to obtain a white solid. The as-synthesized bio-MOF-1 was then dried at room temperature.

Synthesis of MCM-41. MCM-41 powders were prepared following the procedure called "homogeneous precipitation" proposed by Rathousky et al.⁴⁰ A 2.61 g portion (7.161 mmol) of cetyltrimethylammonium bromide (CTAB) was dissolved in 400 mL of water at 30 °C. Then 2.67 g (21.874 mmol) of sodium metasilicate was added. After complete dissolution, 4 mL of ethyl acetate was added with vigorous stirring. After 15 s, the mixture was left in a polypropylene bottle without stirring for 24 h at room temperature. Afterward, a hydrothermal treatment was performed at 100 °C for 48 h. The precipitate was hot filtered, washed with ethanol and water (3×10 mL), and dried at room temperature. Finally, the product was calcined at 600 °C for 20 h (heating rate 1 °C min^{-1}).

Synthesis of SBA-15. The porous material SBA-15 was prepared following the procedure proposed by Zhao et al.⁴¹ A 2 g portion of Pluronic 123 (poly(ethylene glycol)-*block*-poly(propylene glycol)-*block*-poly(ethylene glycol), $(\text{EO})_{20}(\text{PO})_{70}(\text{EO})_{20}$, molecular weight 5800; EO = ethylene oxide, PO = propylene oxide) was dissolved with stirring in 104 mL of water and 20 mL of HCl 37% solution at room temperature. After adding 7.4 mL (20.3 mmol) of tetraethyl orthosilicate (TEOS), the resultant solution was kept at 40 °C for 20 h. The slurry was then hydrothermally treated at 100 °C for 24 h. The product was filtered, washed with water, dried at room temperature, and finally calcined in air at 550 °C for 6 h (heating rate 1 °C min^{-1}).

Synthesis of MCM-41- SO_3H . The SO_3H -functionalized MCM-41 was prepared according to the previously described method.³⁷ The calcined powder MCM-41 was functionalized with thiol groups by silylation with 3-mercaptopropyltrimethoxysilane (MPTMS). In a typical synthesis, 0.5 g of powder was placed in a Schlenk flask that was then evacuated for several hours. The flask was filled with argon and the powder was suspended in 20 mL of dichloromethane at 0 °C. To this suspension was added 1.86 mL of MPMS (20 mmol g^{-1}), and the mixture was stirred for 22 h under an argon atmosphere. During this treatment, the cooling bath was not renewed. The resulting suspension was filtered, washed with dichloromethane and ethanol (3×10 mL), and dried at 100 °C for 5 h. Subsequent oxidation of the attached thiol groups with H_2O_2 led to sulfonic acid functionalized powders. In a typical oxidation 0.3 g of thiol functionalized powder was suspended in 10 mL of H_2O_2 (30 wt %) and stirred for 48 h at room temperature. The product was filtered and washed with ethanol and water. The still wet solid was then suspended in 30 mL of H_2SO_4 (1 M) and stirred

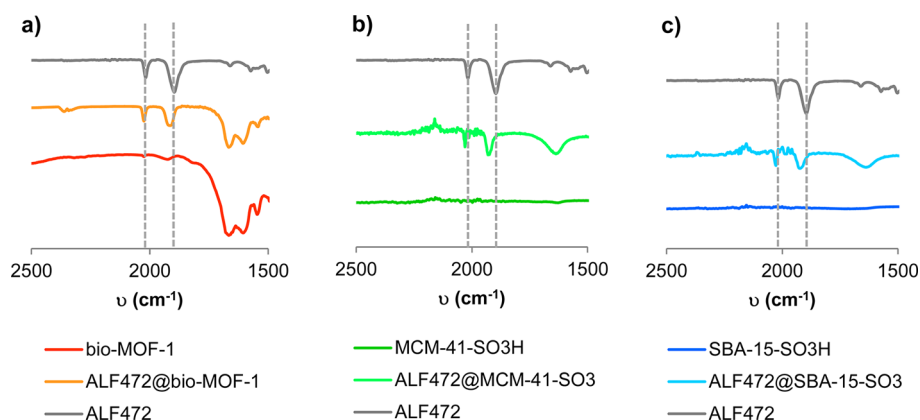


Figure 2. CO stretching region of the FTIR spectra of $[\text{Mn}(\text{tacn})(\text{CO})_3]^+$ (ALF472^+), demonstrating the successful encapsulation of the cationic CORM into the host anionic porous matrixes by a cation exchange process: (a) $\text{ALF472}@$ bio-MOF-1; (b) $\text{ALF472}@$ MCM-41-SO₃; (c) $\text{ALF472}@$ SBA-15-SO₃.

for 2 h at room temperature. Filtration and washing with ethanol and water (3×10 mL) were the final steps to obtain the functionalized material MCM-41-SO₃H. Anal. Calcd for $\text{SiO}_2[(\text{CH}_2)_3\text{SO}_3\text{H}]_{0.023}(\text{H}_2\text{O})_{0.18}(\text{CH}_3\text{CH}_2\text{OH})_{0.05}$: C, 3.04; H, 1.02; S, 0.98. Found: C, 2.96; H, 1.21; S, 1.07.

Synthesis of SBA-15-SO₃H. The synthesis of SBA-15-SO₃H was prepared as reported.³⁸ A 4 g portion of Pluronic 123 (poly(ethylene glycol)-*block*-poly(propylene glycol)-*block*-poly(ethylene glycol)), (EO)₂₀(PO)₇₀(EO)₂₀, molecular weight 5800; EO = ethylene oxide, PO = propylene oxide) was dissolved with stirring in 125 g of 1.9 M HCl solution at room temperature. After the addition of 7.4 mL (32.8 mmol) of tetraethyl orthosilicate (TEOS), the resultant solution was equilibrated for 3 h for prehydrolysis, and then 8.2 mmol of MPTMS and 73.8 mmol of H₂O₂ were added to the solution. The resulting mixture was stirred at 40 °C for 20 h and then transferred into a polypropylene bottle and kept for 24 h at 100 °C (aging process). Afterward, the template was removed from the as-synthesized material by refluxing in ethanol for 24 h (1.5 g of as-synthesized material per 400 mL of ethanol), filtering, washing with separate portions of water and ethanol, and drying at room temperature, yielding the extracted SBA-15-SO₃H. Anal. Calcd for $\text{SiO}_2[(\text{CH}_2)_3\text{SO}_3\text{H}]_{0.14}(\text{H}_2\text{O})_{0.15}(\text{CH}_3\text{CH}_2\text{OH})_{0.07}$: C, 8.18; H, 2.05; S, 5.34. Found: C, 8.08; H, 2.06; S, 5.39.

Guest Material Characterization. (1,4,7-Triazacyclononane)tricarbonylmanganese(I) bromide, $[\text{Mn}(\text{C}_6\text{N}_3\text{H}_{15})(\text{CO})_3]\text{Br}$ (ALF472), was prepared by Alfa Ltd. according to the method previously described by Wieghardt.³⁵ The analytically pure compound has two strong absorptions in the FTIR spectrum at ν_{CO} 2017 and 1895 cm^{-1} (Figure 2). The compound is soluble in water (5 mg mL^{-1}). Solutions are stable in the dark up to 24 h. The compound releases CO upon light irradiation (see below). It is not toxic to RAW264.7 macrophages up to 100 μM concentrations, as determined by the standard MTT assay (see below).

Cytotoxicity Assay. Murine RAW264.7 monocyte macrophages were obtained from the European Collection of Cell Cultures (ECACC 91062702; Salisbury, Wiltshire, U.K.) and cultured in Dulbecco's modified Eagle's medium (cat. 41966029, Gibco, Invitrogen) supplemented with 10% fetal bovine serum (cat. 10500064, Gibco, Invitrogen). Cultures were maintained at 37 °C in a 5% CO₂ humidified atmosphere. The RAW264.7 macrophages were incubated in the presence of complex ALF472 (at a concentration of 10, 50, or 100 μM) for 24 h. The culture medium was replaced by fresh culture medium supplemented with 1 mg/mL of MTT (3-(4,5-dimethyl-2-thiazolyl)-2,5-diphenyl-2H-tetrazolium bromide; A2231, AppliChem). Cells were incubated under the same conditions for 1 h. The culture medium was discarded, and the formazan crystals were solubilized in dimethyl sulfoxide. The absorbance of the solutions was measured at 550 nm in a BioRad Microplate Reader. The percentage

of survival was calculated by considering the growth of the cells in culture medium alone as 100%.

Evacuation/Activation of MCM-41-SO₃H and SBA-15-SO₃H.

Prior to the loading of ALF472, the mesoporous silica materials (MCM-41-SO₃H and SBA-15-SO₃H) were outgassed (10^{-4} bar, 60 °C) for 5 h. Under these conditions, the complete removal of the solvent guest molecules was achieved and empty pores ready for drug adsorption were obtained. Regarding bio-MOF-1, this material was used as synthesized for the prodrug encapsulation.

Chemical Stability of Functionalized Porous Materials.

We have performed these tests in the solvent used for the incorporation of the CORM in order to confirm the chemical stability of the empty matrix under the encapsulation conditions. Therefore, the chemical stability of MCM-41-SO₃H and SBA-15-SO₃H was checked in water. In a typical stability study, 100 mg of activated material was suspended in 5 mL of water for 4 days. Then, the solid was filtered, dried, and activated again (60 °C, 5 h under vacuum). A solid-acid titration was performed in order to check the concentration of acidic groups.⁴² Activated material which was not suspended in water was also titrated as a control. In a typical titration experiment, 25 mg of solid sample was added to NaCl aqueous solution (2 M, 10 mL). The resulting suspension was allowed to equilibrate and thereafter was titrated potentiometrically by dropwise addition of 0.01 M NaOH aqueous solution. On the other hand, the chemical stability of bio-MOF-1 was checked in DMF by suspending 70 mg of material in 5 mL of solvent (DMF) for 4 days. Afterward, the solid was filtered off and dried at room temperature before XRPD acquisition.

ALF472 Adsorption in bio-MOF-1 at 25 °C. A 2 mL DMF solution of ALF472 (22.5 mg, 0.084 mmol) was added to a 3 mL DMF suspension of bio-MOF-1 (70 mg, 0.021 mmol, equivalent to 0.042 mmol of exchangeable cationic sites) in darkness with stirring. The mixture was stirred in darkness for 4 days at room temperature in order to ensure that the equilibrium was reached. Then the sample was filtered and the resulting solid was washed with DMF (2×10 mL) and MeOH (1×10 mL) and dried at room temperature. Anal. Calcd for $(\text{NH}_2(\text{CH}_3)_2)_{1.3}[\text{Mn}(\text{C}_6\text{N}_3\text{H}_{15})(\text{CO})_3]_{0.7}[\text{Zn}_8(\text{C}_5\text{N}_3\text{H}_4)_4(\text{C}_{14}\text{H}_8\text{O}_4)_6\text{O}](\text{CH}_3\text{OH})_{1.3}(\text{C}_3\text{H}_7\text{NO})_{10}(\text{H}_2\text{O})_6$: C, 47.51; H, 4.76; N, 12.83. Found: C, 46.97; H, 4.60; N, 13.13. Ratio Zn₈/Mn (EDX): 0.70.

ALF472 Adsorption in MCM-41-SO₃H at 25 °C. The ALF472 solid-liquid adsorption experiments were performed at 25 °C by suspending 100 mg of activated MCM-41-SO₃H ($\text{SiO}_2[(\text{CH}_2)_3\text{SO}_3\text{H}]_{0.02}$, 1.6 mmol, equivalent to 0.03 mmol of exchangeable cationic sites) in a 5 mL aqueous solution of ALF472 (20 mg, 0.06 mmol) in darkness. The mixture was stirred and kept in darkness for 4 days at room temperature in order to ensure that equilibrium was reached. Afterward, the sample was centrifuged (3500 rpm/5 min) and the resulting solid was washed with water (3×6 mL) and dried at room temperature. Anal. Calcd for $\text{SiO}_2[\text{SO}_3(\text{CH}_2)_3\text{Mn}$

(C₆N₃H₁₅)(CO)₃]_{0.015}(H₂O)_{0.75}(CH₃CH₂OH)_{0.05}: C, 4.23; H, 2.79; N, 0.83; S, 0.56. Found: C, 4.14; H, 2.61; N, 0.78; S, 0.59. Ratio Si/Mn (EDX): 0.015.

ALF472 Adsorption in SBA-15-SO₃H at 25 °C. The ALF472 solid–liquid adsorption experiments were performed at 25 °C by suspending 100 mg of the activated SBA-15-SO₃H (SiO₂[(CH₂)₃SO₃H]_{0.14}, 1.3 mmol, equivalent to 0.18 mmol of exchangeable cationic sites) in a 5 mL aqueous solution of ALF472 (124 mg, 0.36 mmol) in darkness. The mixture was stirred in darkness for 4 days at room temperature in order to ensure that the equilibrium was reached. Then the sample was centrifuged (3500 rpm/5 min) and the resulting solid was washed with water (3 × 6 mL) and dried at room temperature. Anal. Calcd for SiO₂[(CH₂)₃SO₃H]_{0.045}[SO₃(CH₂)₃Mn(C₆N₃H₁₅)(CO)₃]_{0.044}(H₂O)_{0.6}: C, 8.33; H, 2.14; N, 1.79; S, 3.20. Found: C, 8.56; H, 2.63; N, 1.97; S, 3.05. Ratio Si/Mn (EDX): 0.044.

Stability Studies of the Hybrid Materials in Water. Suspensions of ALF472@bio-MOF-1, ALF472@MCM-41-SO₃, and ALF472@SBA-15-SO₃ (concentration based on 10 μM of ALF472) were kept in water under visible light at 37 °C for 7, 24, and 72 h. At each time, the samples were centrifuged and the supernatant was collected and filtered off (Nylon filter membrane, 0.2 μm). The concentration in the supernatant of the elements of interest (Zn and Mn in the case of ALF472@bio-MOF-1 and Si and Mn for the hybrid silica materials) were determined by ICP-OES.

Stability Studies of the Hybrid Materials in PBS. In order to evaluate the cation exchange in PBS of the ALF472 in the hybrid materials, 5 mg of ALF472@MCM-41-SO₃ and ALF472@SBA-15-SO₃ were suspended in 1 mL of PBS (10 mM) for 1, 6, and 24 h in darkness at room temperature. At each time, the suspensions were centrifuged and the supernatant was collected to determine the concentration of ALF472 leached by UV–visible spectroscopy (λ 345 nm). In the case of bio-MOF-1, the leaching in PBS was not evaluated, as the matrix already degrades completely in water (see Results and Discussion).

Determination of CO Release by Myoglobin Assay. The amount of released CO was monitored as previously reported.^{43,44} The CO release from ALF472 and the loaded materials ALF472@bio-MOF-1, ALF472@SBA-15-SO₃, and ALF472@MCM-41-SO₃ was studied spectrophotometrically by measuring the conversion of deoxy-myoglobin (deoxy-Mb) to carbonmonoxy-myoglobin (Mb-CO). The amount of Mb-CO formed was quantified by measuring the absorbance at 423 nm at different times. Stock solutions of myoglobin from equine heart (100 μM, adjusted by UV–visible spectroscopy), sodium dithionite (40 mg mL⁻¹), ALF472 (1 mM), and stock suspensions of the CO-releasing materials (1 mM, based on ALF472) were freshly prepared in degassed phosphate buffered saline (PBS, 0.01 M, pH = 7.4). A 100 μL portion of myoglobin stock solution, 100 μL of sodium dithionite stock solution, 790 μL of degassed PBS, and 10 μL of ALF472 stock solution or CO-releasing material stock suspensions (ALF472@bio-MOF-1, ALF472@SBA-15-SO₃, and ALF472@MCM-41-SO₃) were placed in a sealed quartz cuvette (1400 μL) under an inert atmosphere and kept at 37 °C under visible light for 24 h (using a fluorescent lamp; luminous flux 600 lm; color temperature 4000 K, distance between lamp and cuvette 5 cm). The solutions were analyzed by means of UV–vis at different times (0, 15, 30, 60, 90, 120, 150, 180, 240, 300, 360, 480, 600, 720, and 1440 min) in order to determine the released amount of CO and the kinetics of the process. After 24 h, the solutions were bubbled with CO and the concentration of Mb-CO was calculated as previously reported.⁴⁴ Additional CO-releasing assays of free ALF472 (10 μM) were performed in order to confirm that the CO release only takes place after activation with visible light and to evaluate the influence of free adenine (57 μM) in its CO delivery rate. The adenine concentration corresponds to that leached after the complete degradation of bio-MOF-1. All experiments were performed in triplicate.

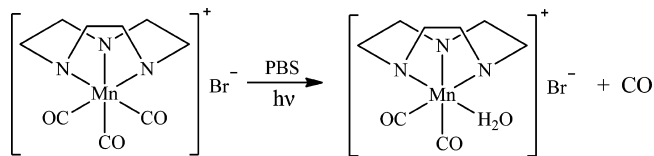
Characterization. N₂ adsorption isotherms were measured at 77 K on a Micromeritics Tristar 3000 volumetric instrument. Prior to measurement powdered silica samples (MCM-41-SO₃H and SBA-15-

SO₃H) were activated by heating at 60 °C for 5 h and outgassing to 10⁻⁴ bar. UV–vis spectra were collected on a Shimadzu UV spectrophotometer. XRPD data were collected on a Bruker D2-PHASE diffractometer (2θ) using Cu Kα radiation (λ = 1.5418 Å) and a LYNXEYE detector, from 5 to 30° (2θ) with a step size of 0.02°. The compounds were manually ground in an agate mortar and then deposited in the hollow of a silicon sample holder. Elemental (C, H, N, S) analyses were obtained with a Flash EA1112 CHNS-O instrument (Centre of Scientific Instrumentation of the University of Jaen). Thermogravimetric analyses were performed using a Mettler Toledo TGA/DSC STAR system under oxygen flow (20 mL min⁻¹) running from room temperature to 900 °C with a heating rate of 2 °C min⁻¹ (Centre of Scientific Instrumentation of the University of Granada). Inductively coupled plasma optic emission spectrometry analysis (ICP-OES) was carried out with an OPTIMA 7300 DV instrument (SCAI, University of Malaga). The attenuated total reflectance (ATR) data were collected with a Bruker Tensor 25 Fourier transform infrared spectrophotometer, using the Gladiater attenuated total reflectance accessory. The ¹H NMR spectra were recorded with a Varian INOVA UNITY 300 MHz NMR spectrometer (Centre of Scientific Instrumentation of the University of Granada). Energy-dispersive X-ray spectroscopy (EDX) analyses were performed using a STEM PHILIPS CM20 HR microscope equipped with an EDX spectrometer operating at an accelerating voltage of 200 keV (Centre of Scientific Instrumentation of the University of Granada). Samples were prepared by dispersing a small amount of the material (3 mg) in absolute ethanol (1 mL) followed by sonication for 10 min and deposition on a copper grid.

RESULTS AND DISCUSSION

Synthesis and Characterization. The ALF472 CORM, which was provided by Alfama Ltd., is an air-stable and water-soluble manganese complex (Scheme 1). In addition, it is stable

Scheme 1. Proposed Visible Light Photoactivation of the [Mn(tacn)(CO)₃]Br (ALF472) CORM under Simulated Physiological Conditions



in the dark and its potential biological application seems not to be hampered by toxicity issues, since it is not toxic to RAW246.7 macrophages in concentrations up to 100 μM (Figure S1 in the Supporting Information).

The porous materials bio-MOF-1,³⁶ MCM-41,⁴⁰ and SBA-15⁴¹ were also prepared according to the literature methods. The functionalization of the silica matrices with propylsulfonic groups was successfully achieved,^{37,38} leading to MCM-41-SO₃H (Si/SO₃H molar ratio: 1/0.023) and SBA-15-SO₃H (Si/SO₃H molar ratio: 1/0.14). All materials were characterized by elemental analysis (EA), infrared spectroscopy (IR), thermogravimetric analysis (TG), and N₂ adsorption at 77 K. The phase purity of bio-MOF-1 was also confirmed by XRPD (Figure S2 in the Supporting Information). The nitrogen adsorption/desorption isotherms of the nonfunctionalized silica compounds showed BET surface areas similar to those previously reported (MCM-41, 885 m² g⁻¹; SBA-15, 700 m² g⁻¹). As expected, the functionalization of the silica materials resulted in a slight decrease of porosity (MCM-41-SO₃H, 825 m² g⁻¹; SBA-15-SO₃H, 675 m² g⁻¹; Figure S3 in the Supporting Information).

ALF472 Incorporation. We have evaluated the applicability of the anionic matrixes (bio-MOF-1 and functionalized silicas) for the encapsulation of ALF472 in order to test the suitability of these new hybrid materials for the controlled delivery of CO. With this aim, we incorporated ALF472 into the porous matrixes by means of cation exchange in DMF (bio-MOF-1) or H₂O (functionalized silicas). In all cases, the porous matrixes were suspended for 4 days in a solution containing the double-stoichiometric amount of ALF472 with regard to the available exchangeable extraframework cations. All of the encapsulations were performed at room temperature and in darkness to avoid the photoactivation of the CORM (see the [Experimental Section](#)). Finally, the suspensions were filtered and washed with DMF and MeOH (bio-MOF-1) or H₂O (functionalized silicas), giving rise to the loaded matrixes ALF472@bio-MOF-1, ALF472@MCM-41-SO₃, and ALF472@SBA-15-SO₃.

The successful incorporation of the CO-releasing molecule inside the porous materials was first confirmed by infrared spectroscopy ([Figure 2](#)). The characteristic stretching CO bands of ALF472 appear slightly shifted in the hybrid materials in comparison to the pristine CORM (from ν 2017 cm⁻¹ to 2030 cm⁻¹ and from ν 1895 cm⁻¹ to 1925 cm⁻¹). This small displacement may be related to the confinement of the CORM molecules inside the pores, as previously reported in the literature.³⁴ The quantification of the amount of encapsulated CORM was determined by energy-dispersive X-ray spectroscopy (ALF472@bio-MOF-1, Zn/Mn = 1/0.088; ALF472@MCM-41-SO₃, Si/Mn = 1/0.015; ALF472@SBA-15-SO₃, Si/Mn = 1/0.044) ([Figure S4](#) in the Supporting Information). Moreover, EDX studies also showed the absence of bromide anions in the hybrid matrixes, which proves the incorporation of ALF472 by a cation exchange process. All of these results were further confirmed by elemental and thermogravimetric analyses ([Figure S5](#) in the Supporting Information). It is worth noting that the silica matrix SBA-15-SO₃H showed the best performance toward the encapsulation of ALF472 with a loading of 0.53 mmol of ALF472⁺ per gram of dried material. This loading represents the exchange of ~50% of the available R-SO₃H sites in the porous matrix. In the case of MCM-41-SO₃H, all of the available R-SO₃H sites (0.22 mmol per gram) were exchanged with the ALF472⁺ cations.⁴⁵ Bio-MOF-1 encapsulated a similar amount of CO prodrug in comparison to MCM-41-SO₃H (0.25 mmol of ALF472⁺ per gram). However, this result accounts only for 35% of the available cationic sites in the MOF framework ([Figure S6](#) in the Supporting Information).

It should be highlighted that the attempts to incorporate ALF472 into the neutral silica frameworks (pristine SBA-15 and MCM-41) were not successful, demonstrating that the encapsulation of the CORM only takes place by a cation exchange process due to the presence of the alkanesulfonic groups. Moreover, this result further confirms the actual encapsulation of the cationic CORM inside the pores of the matrixes rather than its physisorption onto the particle external surface.

In order to evaluate the stability of the selected porous materials under the encapsulation conditions, the empty matrixes were suspended in DMF (bio-MOF-1) or water (silica materials) for 4 days at room temperature. The X-ray powder diffraction studies showed that bio-MOF-1 is recovered unaltered after this treatment, confirming its stability in DMF ([Figure S2](#) in the Supporting Information). On the other hand,

in the case of both functionalized silicas, approximately a third of the alkanesulfonic groups were lost according to the titration assays. The loss of these functional groups was also observed when ALF472 was encapsulated under the same conditions (36% in the case of ALF472@SBA-15-SO₃ and 35% in the case of ALF472@MCM-41-SO₃).

CO Release. The photoinduced CO release properties of ALF472 and the loaded materials, under simulated biological conditions (PBS and 37 °C), were investigated by the myoglobin assay using UV-vis spectroscopy. For this purpose, a PBS solution of equine heart myoglobin was freshly reduced with excess sodium dithionite under nitrogen and then ALF472 or the hybrid materials were added. The CO release rate was followed during 24 h at 37 °C. When kept in the dark, ALF472 does not show spectral changes over 24 h. In contrast, upon irradiation with visible light using a fluorescent lamp (luminous flux 600 lm, color temperature 4000 K), spectral changes characteristic of CO binding to the iron center in the myoglobin were observed in the Soret band, proving that ALF472 is a photoactivable CORM, which can be deduced from the relative decrease and increase in the absorptions at 435 and 423 nm, respectively ([Figure 3](#)).⁴⁴ As previously

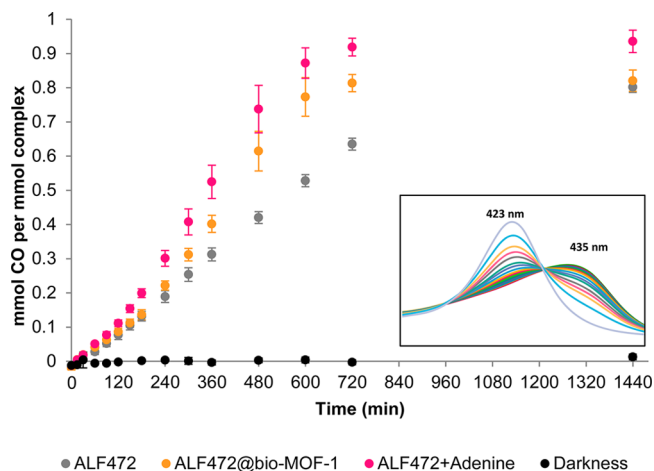


Figure 3. CO delivery kinetics profiles, for ALF472 (gray), ALF472@bio-MOF-1 (orange), and ALF472 + adenine (magenta) under visible light, which suggest a synergistic effect of adenine and visible light in CO release from the photoactive CORM. The black circles indicate the CO release profile in the dark for all cases. The inset shows the evolution of the electronic spectra of myoglobin upon CO coordination. Experimental conditions: Ar atmosphere, PBS, 37 °C, 10 μ M of ALF472, 10 μ M of myoglobin, and 57 μ M of adenine.

reported, in most CORMs, the release of CO from the metal coordination sphere is evoked by ligand exchange reactions with the medium ([Scheme 1](#)).^{46,47} ALF472 releases 0.80 mmol of CO per mmol of complex after 24 h, which proves the higher lability of one of the three CO ligands in each complex. Once ALF472 was incorporated into the ALF472@bio-MOF-1 material, we observed a similar amount of released CO over a 24 h time frame (0.82 mmol of CO per mmol of complex) ([Figure 3](#)). Nevertheless, the CO release kinetics profile of ALF472@bio-MOF-1 matches that of free ALF472 only up to 180 min. It is worth noting that an enhanced CO release rate was observed after 180 min, which might be attributed to the degradation of the MOF matrix with the concomitant leaching of adenine into the solution. In order to confirm the influence of free adenine in the kinetic profile of the CO release from

ALF472@bio-MOF-1, we evaluated the CO delivery rate of a mixture containing free ALF472 and adenine (adenine concentration equal to that provided by the complete degradation of bio-MOF-1). Our results showed that the addition of adenine to a solution of ALF472 enhanced the CO delivery rate upon irradiation, which might be related to the displacement of the labile CO ligand by coordination of the adenine to the metal center, as suggested by ^1H NMR data (Figure S7 in the Supporting Information).

Remarkably, the loaded mesoporous silica materials did slow the CO delivery rate in comparison to the free CORM, which may allow a more controlled CO supply. After 24 h, 0.65 and 0.48 mmol of CO per mmol of encapsulated complex was delivered to the medium for ALF472@MCM-41-SO₃ and ALF472@SBA-15-SO₃, respectively (Figure 4).

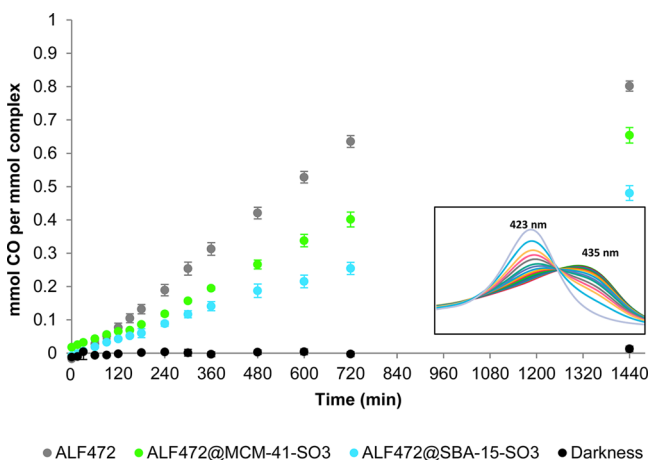


Figure 4. CO delivery kinetics profiles for ALF472 (gray), ALF472@MCM-41-SO₃ (green), and ALF472@SBA-15-SO₃ (blue) under visible light which show the slowing of the CO release rate upon CORM encapsulation. The black circles indicate the CO release profile in the dark for all cases. The inset shows the evolution of the electronic spectra of myoglobin upon CO coordination. Experimental conditions: Ar atmosphere, PBS, 37 °C, 10 μM of ALF472, 10 μM of myoglobin.

Leaching Assays. The leaching of Mn and Zn (bio-MOF-1) or Si (silicas) from the hybrid materials was evaluated in water by inductively coupled plasma optical emission spectrometry (ICP-OES). ALF472@bio-MOF-1 shows an almost complete degradation after 6 h, as 85% of the zinc and 75% of the manganese were detected in the supernatant solution (Table S1 in the Supporting Information). In contrast, silica hybrid materials show robust frameworks, according to the negligible leaching of silicon into the solution (2.9 and 2.2% of Si from MCM-41-SO₃H and SBA-15-SO₃H, respectively, after 24 h). Regarding the leaching of the CORM, 80% of the metal fragments are still kept inside ALF472@MCM-41-SO₃ after 6 h and no further leaching is observed up to 72 h. In the case of ALF472@SBA-15-SO₃, 57% of the manganese complex remains encapsulated after 6 h with an additional slight decrease of ca. 11% after 3 days (Table S1 in the Supporting Information). The higher residence of ALF472 inside the pores of MCM-41-SO₃H may be related to the narrower size of its channel windows in comparison to SBA-15-SO₃H, which may hamper the diffusion of the prodrug. According to these results, for a potential topical application, ALF472@MCM-41-SO₃ can be considered the most promising material, as stable aqueous suspensions can be prepared in the dark.

With the aim of evaluating the potential use of these systems for topical CO release activated by visible light, we decided to further study the leaching of the prodrug under simulated physiological conditions (PBS). The assays were performed in darkness to avoid the decarbonylation process. While 85% of the prodrug was released after 1 h from ALF472@MCM-41-SO₃, only 52% was leached from ALF472@SBA-15-SO₃, reaching a maximum of 75% after 24 h (Table S2 in the Supporting Information). This different behavior seems to be related to the presence of free alkanesulfonic groups in ALF472@SBA-15-SO₃, which may favor the permanence of ALF472 inside the channels, slowing down the cation exchange rate in PBS. On the other hand, the faster delivery of the CORM into the physiological medium from these loaded functionalized silicas, in comparison with pure water, is probably due to a cation exchange process, since a high salt concentration is present in PBS. For topical applications, such a cation exchange process under physiological conditions may allow a better contact of the prodrug with the skin and, subsequently, a more efficient light-induced CO release. As previously mentioned, the use of photoactive CORMs paves the way for the development of new anticancer topical therapies.²³

CONCLUSIONS

The encapsulation of the photoactive, nontoxic, water-soluble, and air-stable cationic CORM [Mn(tacn)(CO)₃]⁺ (ALF472⁺) into different inorganic anionic porous matrixes can be accomplished by a simple cation exchange strategy. The results show that the best performance is achieved by the anionic silica matrixes, which slow the kinetics of the release of CO, allowing a more controlled CO supply. In contrast, the instability of the bio-MOF-1 system, under physiological conditions, leads to the complete leaching of the CORM. For this reason, this hybrid material shows a CO kinetic profile similar to that of free CORM at short times. Nevertheless, after the complete degradation of the MOF matrix, an enhanced CO release rate was observed, which seems to be related to the presence of free adenine in the solution.

The photoactive behavior of the ALF-472@hybrid silica-SO₃ materials may allow the development of on–off switch delivery systems, which ultimately may exert a control over the timing and amount of released CO. This controlled supply of CO could be interesting for phototherapies, such as the topical treatment of skin cancer or other inflammatory skin conditions.

ASSOCIATED CONTENT

Supporting Information

The Supporting Information is available free of charge on the ACS Publications website at DOI: 10.1021/acs.inorgchem.6b00674.

XRP diffractograms, thermogravimetric and EDX analyses, cytotoxicity studies, nitrogen adsorption isotherms, ^1H NMR, and additional data from leaching assays (PDF)

AUTHOR INFORMATION

Corresponding Authors

*E-mail for C.R.M.: crmaldonado@ugr.es.

*E-mail for E.B.: ebaream@ugr.es.

Notes

The authors declare no competing financial interest.

ACKNOWLEDGMENTS

The Spanish Ministry of Economy and Competitiveness and UE Feder Program (projects CTQ2014-53486R and CRM Juan de la Cierva Contract), Junta de Andalucía (project P09-FQM-4981 and SR postdoctoral contract) and COST action CM1105 are gratefully acknowledged for generous funding. D.Ch-L thanks the support of the Intramural CSIC project 201530E011. The authors thank Alfama Inc. for providing ALF472. The National NMR Facility is supported by Fundação para a Ciência e a Tecnologia (RECI/BBB-BQB/0230/2012). Project PTDC/QUI-BIQ/117799/2010 provided a grant to H.J.

REFERENCES

- (1) Mann, B. E.; Motterlini, R. *Chem. Commun.* **2007**, No. 41, 4197.
- (2) Foresti, R.; Bani-Hani, M. G.; Motterlini, R. *Intensive Care Med.* **2008**, *34* (4), 649–658.
- (3) Wu, L.; Wang, R. *Pharmacol. Rev.* **2005**, *57* (4), 585–630.
- (4) Marques, A. R.; Kromer, L.; Gallo, D. J.; Penacho, N.; Rodrigues, S. S.; Seixas, J. D.; Bernardes, G. J. L.; Reis, P. M.; Otterbein, S. L.; Ruggieri, R. A.; Gonçalves, A. S. G.; Gonçalves, A. M. L.; Matos, M. N. De; Bento, I.; Otterbein, L. E.; Blättler, W. A.; Romão, C. C. *Organometallics* **2012**, *31* (16), 5810–5822.
- (5) Boczkowski, J.; Poderoso, J. J.; Motterlini, R. *Trends Biochem. Sci.* **2006**, *31* (11), 614–621.
- (6) Romão, C. C.; Blättler, W. A.; Seixas, J. D.; Bernardes, G. J. L. *Chem. Soc. Rev.* **2012**, *41* (9), 3571–3583.
- (7) Clark, J. E. *Circ. Res.* **2003**, *93* (2), 2e–8.
- (8) Motterlini, R.; Mann, B. E. Preparation of metal complexes for therapeutic delivery of carbon monoxide as vasodilator. WO 2002/092075, 2002.
- (9) Alberto, R.; Motterlini, R. *Dalton Trans.* **2007**, No. 17, 1651–1660.
- (10) Vummaleti, S. V. C.; Branduardi, D.; Masetti, M.; De Vivo, M.; Motterlini, R.; Cavalli, A. *Chem. - Eur. J.* **2012**, *18*, 9267–9275.
- (11) Nagel, C.; McLean, S.; Poole, R. K.; Braunschweig, H.; Kramer, T.; Schatzschneider, U. *Dalton Trans.* **2014**, *43*, 9986–9997.
- (12) Ward, J. S.; Lynam, J. M.; Moir, J. W. B.; Sanin, D. E.; Mountford, A. P.; Fairlamb, I. J. S. *Dalt. Trans.* **2012**, *41* (35), 10514–10517.
- (13) Ward, J. S.; Lynam, J. M.; Moir, J.; Fairlamb, I. J. S. *Chem. - Eur. J.* **2014**, *20* (46), 15061–15068.
- (14) Kretschmer, R.; Gessner, G.; Görls, H.; Heinemann, S. H.; Westerhausen, M. J. *Inorg. Biochem.* **2011**, *105* (1), 6–9.
- (15) Chaves-Ferreira, M.; Albuquerque, I. S.; Matak-Vinkovic, D.; Coelho, A. C.; Carvalho, S. M.; Saraiva, L. M.; Romão, C. C.; Bernardes, G. J. L. *Angew. Chem., Int. Ed.* **2015**, *54* (4), 1172–1175.
- (16) Zobi, F.; Blacque, O.; Jacobs, R. A.; Schaub, M. C.; Bogdanova, A. Y. *Dalt. Trans.* **2012**, *41* (2), 370–378.
- (17) Abraham, N. G.; Kappas, A. *Pharmacol. Rev.* **2008**, *60* (1), 79–127.
- (18) Parfenova, H.; Leffler, C. W. *Curr. Pharm. Des.* **2008**, *14* (5), 443–453.
- (19) Motterlini, R.; Otterbein, L. E. *Nat. Rev. Drug Discovery* **2010**, *9* (9), 728–743.
- (20) Leffler, C. W.; Parfenova, H.; Jaggar, J. H. *Am. J. Physiol. Heart Circ. Physiol.* **2011**, *301*, H1–H11.
- (21) Gullotta, F.; Di Masi, A.; Ascenzi, P. *IUBMB Life* **2012**, *64* (5), 378–386.
- (22) Sandouka, A.; Fuller, B. J.; Mann, B. E.; Green, C. J.; Foresti, R.; Motterlini, R. *Kidney Int.* **2006**, *69* (2), 239–247.
- (23) Allanson, M.; Reeve, V. E. *Cancer Immunol. Immunother.* **2007**, *56* (11), 1807–1815.
- (24) Schatzschneider, U. *Inorg. Chim. Acta* **2011**, *374* (1), 19–23.
- (25) Hasegawa, U.; Van Der Vlies, A. J.; Simeoni, E.; Wandrey, C.; Hubbell, J. A. *J. Am. Chem. Soc.* **2010**, *132* (51), 18273–18280.
- (26) Dördelmann, G.; Pfeiffer, H.; Birkner, A.; Schatzschneider, U. *Inorg. Chem.* **2011**, *50* (10), 4362–4367.
- (27) Dördelmann, G.; Meinhardt, T.; Sowik, T.; Krueger, A.; Schatzschneider, U. *Chem. Commun.* **2012**, *48*, 11528–11530.
- (28) Kunz, P. C.; Meyer, H.; Barthel, J.; Sollazzo, S.; Schmidt, A. M.; Janiak, C. *Chem. Commun. (Cambridge, U. K.)* **2013**, *49*, 4896–4898.
- (29) Bohlender, C.; Gläser, S.; Klein, M.; Weisser, J.; Thein, S.; Neugebauer, U.; Popp, J.; Wyrwa, R.; Schiller, A. *J. Mater. Chem. B* **2014**, *2* (11), 1454–1463.
- (30) Ma, M.; Noei, H.; Mienert, B.; Niesel, J.; Bill, E.; Muhler, M.; Fischer, R. A.; Wang, Y.; Schatzschneider, U.; Metzler-Nolte, N. *Chem. - Eur. J.* **2013**, *19*, 6785–6790.
- (31) Vallet-Regí, M.; Balas, F.; Arcos, D. *Angew. Chem., Int. Ed.* **2007**, *46* (40), 7548–7558.
- (32) Manzano, M.; Vallet-Regí, M. *J. Mater. Chem.* **2010**, *20* (27), 5593–5604.
- (33) Capelli, C. C.; Dennis, A. P. Devices and methods for inhibiting fibrosis. WO 2008/080128, 2008.
- (34) Gonzales, M. A.; Han, H.; Moyes, A.; Radinos, A.; Hobbs, A. J.; Coombs, N.; Oliver, S. R. J.; Mascharak, P. K. *J. Mater. Chem. B* **2014**, *2*, 2107–2113.
- (35) Pomp, C.; Drüeke, S.; Küppers, H. J.; Wieghardt, K. Z. *Naturforsch., B: J. Chem. Sci.* **1988**, *43*, 299–305.
- (36) An, J.; Geib, S. J.; Rosi, N. L. *J. Am. Chem. Soc.* **2009**, *131* (24), 8376–8377.
- (37) Marschall, R.; Bannat, I.; Caro, J.; Wark, M. *Microporous Mesoporous Mater.* **2007**, *99* (1–2), 190–196.
- (38) Shen, J. G. C.; Herman, R. G.; Klier, K. J. *Phys. Chem. B* **2002**, *106* (39), 9975–9978.
- (39) Pore diameters of MCM-41-SO₃H and SBA-15-SO₃H were calculated by the BJH method.
- (40) Rathouský, J.; Zukalová, M.; Zukal, A.; Had, J. *Collect. Czech. Chem. Commun.* **1998**, *63* (11), 1893–1906.
- (41) Zhao, D.; Feng, J.; Huo, Q.; Melosh, N.; Fredrickson, G.; Chmelka, B.; Stucky, G. *Science* **1998**, *279* (5350), 548–552.
- (42) Shen, J. G. C.; Kalantar, T. H.; Herman, R. G.; Roberts, J. E.; Klier, K. *Chem. Mater.* **2001**, *13*, 4479–4485.
- (43) Motterlini, R.; Clark, J. E.; Foresti, R.; Sarathchandra, P.; Mann, B. E.; Green, C. J. *Circ. Res.* **2002**, *90* (2), e17–e24.
- (44) Bikiel, D. E.; González Solveyra, E.; Di Salvo, F.; Milagre, H. M. S.; Eberlin, M. N.; Corrêa, R. S.; Ellena, J.; Estrin, D. a; Doctorovich, F. *Inorg. Chem.* **2011**, *50* (6), 2334–2345.
- (45) Calculated on the basis of the SO₃H groups present in the matrix after the encapsulation treatment.
- (46) Schatzschneider, U. *Br. J. Pharmacol.* **2015**, *172* (6), 1638–1650.
- (47) Marhenke, J.; Trevino, K.; Works, C. *Coord. Chem. Rev.* **2016**, *306*, 533–543.